Analytical hybrid effect prediction and evolution of the tensile response of unidirectional hybrid FRP composites for civil engineering applications

Filipe Ribeiro[1], José Sena-Cruz[2], Fernando G. Branco[3], Eduardo Júlio[4], Fernando Castro[5]

[1] PhD Student, CERIS, Instituto Superior Técnico, University of Lisbon, Portugal. E-mail: filipe.t.ribeiro@tecnico.ulisboa.pt

[2] Associate Professor, ISISE, Department of Civil Engineering, University of Minho, Portugal. E-mail: jsena@civil.uminho.pt *Corresponding Author

[3] Assistant Professor, ISISE, Department of Civil Engineering, University of Coimbra, Portugal. E-mail: fjbranco@dec.uc.pt

[4] Full Professor, CERIS, Instituto Superior Técnico, University of Lisbon, Portugal. E-mail: eduardo.julio@tecnico.ulisboa.pt

[5] Full Professor, CT2M, Department of Mechanical Engineering, University of Minho, Portugal. E-mail: fcastro@dem.uminho.pt

Abstract

The performance of a progressive damage model in quantitative hybrid effect prediction of a comprehensive set of different 16 unidirectional interlayer (layer-by-layer) hybrid composites was assessed. Composites, produced by the hand lay-up method, made out of 4 different commercially available dry unidirectional fabric materials, namely high-modulus carbon, standard carbon, E-glass and basalt were tested. Tensile tests on single fibres were performed in order to determine their Weibull strength distribution parameters, which were used as inputs of the progressive damage model. Reasonably good agreement between analytical and experimental hybrid effect results was obtained, which allowed to estimate satisfactorily the reference strengths of the unidirectional low strain composite materials. Next, an existing analytical model for the simulation of stress-strain curve of hybrid composites was adapted to contemplate the hybrid effect, which allowed to predict the following properties of unidirectional hybrid combinations: 'yield' stress (or pseudo-yield stress), pseudo-ductile strain, and strength. It was verified as well that predictions of the three properties referred to were in close agreement with test results. Finally, damage mode maps were used in the analysis of these properties and, furthermore, of the hybrid effect and the elastic modulus of hybrid combinations.

Keywords

Hybrid composites, Hybrid effect, Analytical modelling

Ribeiro, F.; Sena-Cruz, J.; Branco, F.; Júlio, E.; Castro, F. (2020) "Analytical hybrid effect prediction and evolution of the tensile response of unidirectional hybrid FRP composites for civil engineering applications" Journal of Composite Materials, 54(22), 24.

Introduction

The linear elastic behaviour up to the point of sudden brittle failure, without sufficient warning and residual integrity of the traditional unidirectional (UD) Fibre Reinforced Polymers (FRP) composite materials, leads to limitations in the full exploitation of their great inherent mechanical advantages, namely the high tensile strength due to conservative safety design limits [1, 2]. For this reason, the unfavourable failure characteristic of these materials restricts the spread of their application. In this way, the possibility to promote a gradual failure to the composites, improving their safety and maintaining their mechanical virtues simultaneously, has a tremendous interest for different industries, in particular for civil engineering, in which ductile materials are required in several applications (e.g. development of reinforcing bars for RC structures, externally bonded strengthening solutions for RC structures, pultruded profiles for new structures, and cables for long-span bridges). In fact, the possibility of avoiding tensile catastrophic failure with composites entirely constituted by brittle materials is one of the major advantages of hybridisation, since the latter can effectively contribute to increase structural safety. This is true for different industries, but it has particular interest for civil engineering. In this industry, it is common to apply composites as reinforcing bars for RC structures or as externally bonded strengthening solutions for reinforcing concrete (RC) structures. As it is known, RC has the potential of resisting significant tensile stresses, unlike plain concrete, since the reinforcing steel bars provide ductility to the concrete RC members that otherwise would exhibit a brittle behaviour. In practical terms, this implies that, if a properly reinforcing concrete element were to fail in tension, then such a failure would, fortunately, be preceded by large displacement caused by the yielding of steel reinforcing bars, thereby giving ample warning of the impending collapse. Thus, it is seem seen with great interest the possibility of applying hybrid composite (pseudo-ductile) on concrete elements (fragile). As it is known, composite materials have superior mechanical strength advantage and they have better potential durability when compared with steel. For this reason, their use may provide more cost-effective solutions in civil engineering applications.

Hybridisation, defined as the incorporation of two fibre types with different strain failures, usually designated as Low Strain (LS) and High Strain (HS) fibres, within the same polymeric matrix [3], allows overcoming the lack of ductility. With this innovative solution, it is possible to achieve a mechanical non-linear and non-catastrophic behaviour characterized by presenting a flat-topped stress-strain curve in monotonic tensile tests. This desired behaviour is reached by selecting appropriate relative thickness of the involved materials (i.e. proportion of the LS to HS material layers) and absolute thickness of the LS material layers. It is important to note that achieving non-catastrophic behaviour is possible with some configuration of UD hybrid composites, by selecting appropriate relative thickness of the involved materials (i.e. proportion of the LS to HS material layers) and absolute thickness of the LS material layers. However, if the hybrid configuration is not carefully designed, because of the delamination propagation, the hybrid composite may break suddenly. Additionally, it can also shows a lower strength than the individual constituents. Non-catastrophic behaviour hybrid composites is not repeatable on subsequent unloadings/reloadings. In this context, this behaviour is known as pseudo-ductile [4, 5]. Pseudo-ductile behaviour is characterized by fragmentation of the LS fibres and dispersed delamination of the LS fibres fragments from the undamaged high strain HS fibres.

In addition to the potential to introduce pseudo-ductility to the UD composite materials, hybridisation promotes synergies between the involved reinforcing materials, leading, for instance, to the increase (until 50% [5, 6]) of the apparent failure strain of LS fibres. This phenomenon has been described as "hybrid effect" and it was reported, for the first time, in 1972, by Hayashi [7]. Today, there is some controversy about the best way how to define the baseline tensile failure strain of a UD non-hybrid composite, against which, the strain at failure of the hybrid composite is compared in the determination of the hybrid effect. In standard tensile tests of UD non-hybrid composites, stress concentrations can arise where the load is applied 8, leading to the reduction of the baseline strain. This effect can lead to premature failures and may be responsible for some of the variability observed in tensile results, published worldwide. It should be noted that, according to standards (e.g. EN 527-5), clamping system shall not cause premature facture at the grips. However, the information about the failure mode is not referred to in many works. This leads to difficulties in interpreting the results. A potential specimen type to suppress premature failures

is presented in [8]. However, the proposed specimen type is not yet widely widespread.

Swolfs *et al.* [5] pointed out changes in three main mechanisms as cause of hybrid effect: (1) residual thermal stresses, (2) fracture propagation effects and (3) dynamic stress concentrations. Relatively to the first change, in a more recent work, Sowlfs *et al.* [9] state that using representative thermal expansion coefficients and longitudinal Young's moduli of fibres, the influence of residual thermal stresses in hybrid effect is small for carbon/glass hybrid composites. Wisnom *et al.* [8] supported the previous view, mentioning that a low effect of thermal residual stresses would be expected in UD hybrid composites, where stresses are driven by the difference in fibre expansion coefficients rather than by matrix contraction. Relatively to the second change, it is possible to understand that hybridisation can modify the stress concentrations and stress recovery at a broken fibre due to the presence of neighbouring fibres with different stiffness [10]. In fact, it is believed that substantial increase in strain of the LS fibres is caused by the restraint from the adjacent HS fibres, which inhibits the formation of broken clusters of LS material [8]. Relatively to the third change, it has been poorly investigated in the past two decades [5, 8]. Finally, in addition to the 3 main changes cited before, the size effect has also been shown to influence the hybrid effect [6, 8, 9]. This fact is understandable because, for a constant sample size, the number of LS fibres is reduced by the hybridisation, leading to lower probability of finding a flaw and, consequently, to superior strains at the failure of LS fibres in hybrid composites. Nevertheless, the magnitude of the size effect is not quantified [9].

Over time, different analytical models to predict the mechanical response of UD hybrid composites have been developed. Zweben [11], in 1977, extended a previous developed shear lag model for UD non-hybrid composites. This model assumes that fibres carry all the axial load and the matrix only the shear load. A strain concentration factor is responsible to increase the stress in the HS fibre next to a single LS broken fibre. It is assumed that a broken LS fibre locally loses its load transfer capacity over a certain length, by the definition of an ineffective length. Later, Fukuda [12], in 1983, improved Zweben's model, introducing more accurate stress concentration factors and ineffective lengths and turning the model independent to the ratio of failure strains between fibres. One of the most relevant disadvantages of the models of Zweben [11] and Fukuda [12] is that they consider a fixed ratio of LS over HS fibres, which means that it is not possible to check the influence of the variation of LS fibres relative volume fraction (vol%) with these models. This parameter is a crucial factor on mechanical hybrid response [6, 9, 13].

In last years, Global Load Sharing (GLS) theory, developed by Curtin [14, 15] and expanded by Hui *et al.* [16] for UD non-hybrid composites, has been adapted for UD hybrid composites [9, 17, 18]. GLS incorporates the mechanics and statistics of fibre fragmentation and assumes that the stress dropped by a broken fibre is redistributed equally to all other fibres in the plane of the break [17]. Analytical models based on GLS theory, sometimes referred to as Progressive Damage Models (PDMs) [19], should be able to reproduce the on-axis non-linear behaviour of a UD composites, where the mechanical properties are fibre-dominated. Although the GLS theory omits many real phenomena, such as fragmentation, local load sharing (stress concentrations), size effects, delamination between composite layers and fibre dispersion, it remains a very useful tool for exploring the effect of constituent properties on the composite performance [17]. In fact, if the shear yield strength of the matrix is sufficiently low, then the local stress concentrations cannot be too large and the stress must be redistributed over a large number of fibres [15]. Given the analytical nature of the model, there is the advantage of exploring rapidly the hybrid tensile response of different combinations. An extensive revision about GLS theory can be found in [15, 17, 19].

Swolfs *et al.* [9] applied GLS theory in a parametric study of hybrid effect. The developed model allowed the prediction of the hybrid effect of carbon/glass combination. The influence of several factors on the hybrid effect was evaluated, namely the Weibull modulus (see the definition in Weibull fibre strength distribution (input data) section) of carbon fibres and glass fibres, the failure strain ratio, the stiffness ratio and the strength ratio between the involved fibres. It was concluded that hybrid effect is mainly affected by two of the referred to factors: the Weibull modulus of carbon fibres and the stiffness ratio between the fibres. Furthermore, in terms of the strength predictions, it was concluded that the GLS model essentially follows the bilinear rule-of-mixtures (as defined in [5, 20-23]). Rajan and Curtin [17] used as well GLS model to study the tensile response of different UD hybrid combinations of continuous or discontinuous fibres. The analytical model predictions were supported by experimental results obtained in [24]. They concluded that using discontinuous LS fibres improves hybrid composite performance, because such fibres fragment more gracefully over a wide range of strain. However, quantitative

comparisons with experimental results were not presented. Tavares *et al*. [18] extend a PDM, initially developed by Turon *et al*. [19] for UD non-hybrid composites, to UD hybrid composites. An analytical parametric study was performed analysing essentially the influence of the vol% of the constituent materials (3 carbon types and 1 alkali resistant glass) on the tensile response of the resulting hybrid combinations. Through two different models (one that takes into account only the statistical strength distribution of fibre and another that, in addition, considers the influence of the shear yield strength of the matrix) it was possible to conclude that the matrix–fibre interface lead to significant differences in the tensile response. However, a proper justification to this phenomenon (or the identification of pattern) was not reported in the paper.

Despite great progress achieved in last studies with GLS models in hybrid composite, an experimental quantitative validation of fitness of the hybrid effect prediction hasn't been carried out yet consistently [17].

Research in hybrid FRP composites for civil engineering application dates back to the 1990s. At that time, the investigation has been fundamentally focused in the development of three main systems: (i) reinforcing bars for reinforced concrete (RC) structures; (ii) externally bonded strengthening for RC structures, and (iii) pultruded profiles for new structures. More recently, some work has also appeared on the development of cables for long-span bridges. The main motivation for the development of such systems has been the interest by their mechanical performance, i.e., the search for non-abrupt failures. As it is known, large structural deformations and significant load-carrying capacity prior to ultimate failure are critical in civil engineering structures, in which sudden failures are unacceptable. This is import because, in extreme event, it is expected that structures give forewarning of failure and prevent total collapse. As ultimate load is approached, some sections of the structure may reach their ultimate strength before others. In earthquake-resistant design, energy absorption by plastic deformations is necessary for ductile response of structures under seismic loads where load reversal and energy release occur.

Particularly, in retrofitting applications, it is very common to apply composites made in-situ through the hand lay-up method, i.e., forming the composite on the surface of the structural member to be strengthened, using flexible dry fibre fabrics or sheets and liquid adhesives. This has proved to be a cost effective method and, in addition, the composite can adopt versatile shapes and sizes using simple tools. Despite its advantages, the hand lay-up method is dependent on the skill of the worker, and thus quality control plays a major role to ensure that defects and voids are avoided. According to the best practices suggested in the guidelines, e.g. [25], hand lay-up system shall be referred to the area of dry fibres only because, in this case, the final thickness of the composite cannot be deterministically estimated. Since this is a very common manufacturing method of composites in strengthening reinforced concrete structures, analytical models developed to hybrid composites must be validated for civil engineering applications, i.e., considering the specificities of the used the materials, production methods and guidelines.

A first main goal of the present work is to demonstrate that GLS models can be used to estimate the hybrid effect of UD hybrid composites produced with commercial materials intended for civil engineering applications. The focus of this work is to analyse composites manufactured by the hand lay-up method. In this way, the performance of the analytical approach developed recently by Tavares *et al*. [18] was assessed using the experimental results published by the authors in [6]. The statistical strength scatter parameters of the fibres were determined experimentally, through the single fibre tests, to be used as inputs of the model.

Secondly, the model of Jalalvand *et al*. [13] was modified to take into account the hybrid effect predictions obtained with the model of Tavares *et al*. [18]. The evolution of hybrid properties (such as hybrid effect, 'yield' stress, pseudo-ductile strain, elastic modulus and strength) was investigated as function of the configuration of UD hybrid composites by means of novel Damage Mode Maps (DMMs) presented in [26].

Modelling assumptions

Progressive damage model for hybrid composites

The PDM of Tavares *et al.* [18] aims at establishing the degradation of the tensile mechanical properties of the UD hybrid composites resulting from fibre fragmentation that leads to the stiffness-loss simulation of the two constituent reinforcing materials. Traditional brittle fibres used in composites are characterized by their strength scatter due to the presence of flaws introduced during processing and handling. In this way, strength distribution is contemplated in cited PDM, considering the two parameters of Weibull cumulative failure probability distribution, as described in next sections.

Weibull fibre strength distribution (input data)

Fibres are characterized by breaking as soon as the weakest link is overloaded [27]. As most part of physical systems, successive observations of the strength do not produce exactly the same result. In this way, strength of a single fibre cannot be accurate modelled with one single average value. Usually, the strength variable of fibres is described by the Weibull distribution [28]:

$$P(\sigma) = 1 - exp\left(-\left(\frac{L}{L_0}\right)\left(\frac{\sigma}{\sigma_0}\right)^m\right) \quad (1)$$

where L is the characteristic gauge length, L_0 the reference gauge length, σ the fibre strength, σ_0 the Weibull scale parameter and m the Weibull modulus. The Weibull modulus m varies with the scatter around the average value: a large Weibull modulus indicates little scatter in the fibre strength. The reference length L_0 is usually introduced just for convenience, because then L/L_0 becomes a non-dimensional quantity, and the Weibull scale parameter has the dimension of stress. The choice of L and L_0 implies modification of σ_0 parameter value.

The Weibull distribution parameters are usually determined by testing individual fibres, as described in tensile single fibre test section. However, tensile tests of single fibres could be associated to some sources of error, such as specimen alignment with respect to the load direction (that leads to bending stresses in the fibre) and premature fibre failure within the adhesive or at the tabs [29]. Furthermore, the extraction of fibres from a bundle may cause the weakest ones to fracture in the process, thus effectively censoring the fibre sample that undergoes the test [29]. Today, there is a discussion about the best number of tests and the gauge length of specimen, that may influence the estimation of Weibull parameters [27].

Swolfs *et al.* [30] published a detailed literature review about the experimental and statistical issues related with single fibre testing. The fibre preselection, clamping effects, number of tests, gauge length and fibre cross-sectional variation were addressed. It was concluded that, despite many detailed investigations by different researchers, measuring the Weibull distribution remains particularly difficult. Researchers have not yet agreed on the best testing practices. In the present work, as described in tensile single fibre test section, the test setup follows the guidelines laid down in ASTM D3379-75 [31].

In this work, the Weibull distribution parameters from single fibre tests, described in tensile single fibre test, were determined by the maximum likelihood method (MLM) [32], which is believed to be more accurate than least squares regression [27, 32]. However, these values can be seen as susceptible of being altered, according to the sources of error previously reported. The chi-square goodness-of-fit test was used to check distributional assumptions.

Model description

The analytical approach proposed by Tavares *et al.* [18] is an adaptation for UD hybrid composites of the model developed by Turon *et al.* [19]. Essentially, this approach assumes that the fibre fragmentation phenomena of single fibre fragmentation tests (a test in which a single fibre embedded in the matrix is loaded and the number of fibre breaks as a function of the applied load is monitored) has the same nature of the stiffness loss of the UD non-hybrid composite due to fibre breakage. In this way, exactly the same model could be used to predict both behaviours. A synopsis of the model and the underlying assumptions are described as follows.

Ideally, the model considers the behaviour of a single brittle fibre embedded along the centre line of a

dog-bone-shaped matrix specimen, in which the matrix have a much larger cross-sectional area and larger strain to failure than the fibre material. As the strain is increased, the fibre fails progressively at randomly positioned flaws producing an increasing number of shorter fragments. The apparent stiffness of the system, matrix and fibre, decreases with the number of fibre breaks, due to their loss of ability to carry the load. Assuming that the influence of other damage modes (matrix cracking, delamination between plies, and debonding and subsequent pull-out between fibres and the matrix material) is neglected, the number of breaks at a given stress could be related to the apparent axial stiffness of the composite. Equation (2) gives the relationship between the mean number of breaks in a fibre, $\langle N \rangle$, and the length L under a defined σ:

$$\langle N \rangle = \frac{L}{L_0}\left(\frac{\sigma}{\sigma_0}\right)^m \tag{2}$$

When a fibre breaks, the load carried by the fibre drops down to zero at the position of the break, and the load is transferred by shear between the fibre and the matrix. This causes a stress redistribution near fibre break. The model assumes a linear increase of the axial stress from a fibre break, until a total recovery occurs at a certain distance from it. The length of this load recovery region, l_{ex}, is defined as:

$$l_{ex} = \frac{R_f}{\tau}\frac{E_f \varepsilon}{2} \tag{3}$$

where R_f is the fibre radius, E_f is the elastic modulus of fibres, τ the matrix–fibre interfacial shear strength and ε the applied strain.

The average fibre stress along the fibre, σ_m, can be computed by integrating the axial stress over all of the fibre fragments along the fibre length, resulting, after some simplifications (please see the details in [19]), in the following closed-form analytical solution:

$$\sigma_m(\varepsilon) = \left(\frac{1-e^{-2l_{ex}\Lambda}}{2l_{ex}\Lambda} + \Lambda l_{ex} e^{-L\Lambda}\right) E_f \varepsilon \tag{4}$$

where Λ is the number of breaks in a fibre per unit length:

$$\Lambda = \frac{\langle N \rangle}{L} = \frac{1}{L_0}\left(\frac{\sigma}{\sigma_0}\right)^m \tag{5}$$

In case of hybrid composites, the developed model assumes that there are two 'sub-composites' in parallel, one for each reinforcing material, subjected to the same applied axial strain. The model defines how a fibre failure affects the stresses in the remaining intact fibres and assemble the mechanical behaviour of the constituents in the composite material. Given the tensile responses for the two pure composites using GLS (equation (4)), the stress-strain response for the hybrid composite can be described simply by considering the contribution of two materials, taking into account the vol% of the constituents. Damage in the matrix is not considered, since the tensile failure of composite materials is mainly a fibre dominated process [18]:

$$\sigma(\varepsilon) = \left(\left(\frac{1-e^{-2l_{ex,L}\Lambda_L}}{2l_{ex,L}\Lambda_L} + l_{ex,L}\Lambda_L e^{-L\Lambda_L}\right) E_{L,f} V_L + \left(\frac{1-e^{-2l_{ex,H}\Lambda_H}}{2l_{ex,H}\Lambda_H} + l_{ex,H}\Lambda_H e^{-L\Lambda_H}\right) E_{H,f} V_H\right)\varepsilon \tag{6}$$

where $l_{ex,L}$, Λ_L, $E_{L,f}$ and t_L are the length load recovery region, the number of breaks in a fibre per unit length, the elastic modulus and the half thickness of a layer of the LS fibres and $l_{ex,H}$, Λ_H, $E_{H,f}$ and t_H are the length load recovery region, the number of breaks in a fibre per unit length, the elastic modulus and the half thickness of a layer of the HS fibres. V_f is the volume of fibres.

In the present work, the PDM was used to estimate the hybrid effect, defined here as apparent failure strain enhancement of the LS fibre in a hybrid composite compared to the failure strain of a LS fibre-reinforced non-hybrid composite. The failure strain of the LS fibres was considered as the strain at first local maximum point of the stress-strain diagram, see **Figure 1**. However, in some cases, especially in combination with low vol% of LS fibres, a clear local maximum point was impossible to achieve, since the analytical stress-strain diagrams presented only a global maximum point due to statistical issues. This fact is illustrated in the example of **Figure 1** (a): contrary to the case with 50% of HM carbon fibres, in which it is possible to distinguish clearly two local maxima, in the case of 10% of LS fibres, only a global maximum is observable. The lower the volume of LS fibres, the less distinguishable is the first local maximum. This occurs because the contribution of LS fibres to the tensile response of the composite gradually decreases. Although a local maximum is unnoticeable in the analytical stress strain diagrams, certainly hybrid effect exists in combinations with very low vol% of LS fibres. This happens

because the most important factor that influences the hybrid effect is the restraint of clusters formation of break LS fibres due to the adjacent HS material.

Evolution of hybrid properties (damage mode maps)

The effect of the configuration (geometric and material parameters) of hybrid composites on different responses of UD hybrid composites can be clearly interpreted using a novel representation of the damage modes, known as damage mode maps (DMMs), recently developed by Jalalvand *et al*. [26]. The DMMs are a very interesting graphical construction that facilitates interpretation and allows subsequent analysis and better visualization of the evolution of hybrid responses. DMMs have been used [1, 2, 26, 33] to analyse the evolution (through colormaps) of pseudo-ductile strain, defined as the strain between the final failure strain and the strain on the extrapolated initial slope line at the failure stress of the stress-strain diagram, and 'yield' stress, defined as the stress at first local maximum point of stress-strain diagram, of hybrid combinations (see **Figure 2**). In the cited works, the focus was to study the LS layer fragmentation and LS fragmentation and stable delamination damages modes in order to maximize the pseudo-ductile and 'yield' stress. In this way, the DMMs can easily be used as a design tool to achieve optimal hybrid composites with desired damage modes [2]. DMMs divide all possible configurations of a UD hybrid composite into four possible damage modes:

i. Premature HS failure, in which the whole hybrid specimen fails at first LS fracture;
ii. Unstable delamination, in which delamination occurs at first LS fracture;
iii. LS layer fragmentation, in which the energy released at first LS layer is not enough to drive unstable delamination, allowing that other fractures take place in the LS layer until saturation;
iv. LS fragmentation and stable delamination in which the fragmented LS segments are pulled-out stably from the HS layers.

In DMMs, the horizontal axis is the ratio between the thickness of the two fibre type layers and the vertical is the absolute thickness of the LS layer. The boundaries between different zones can be determined by equating any two of the three stress levels described in [13]: (i) the stress level at which the first crack in the LS material occurs, $\sigma@LF$, (ii) the stress level at which delamination development occurs, $\sigma@del$, and (iii) stress level at which the high strain material fails, $\sigma@HF$, in accordance with the equations (7) to (9), respectively.

$$\sigma@LF = S_L \frac{\alpha\beta+1}{\alpha(\beta+1)} \tag{7}$$

$$\sigma@del = \frac{1}{1+\beta}\sqrt{\left(\frac{1+\alpha\beta}{\alpha\beta}\right)\left(\frac{2G_{IIC}E_H}{t_H}\right)} \tag{8}$$

$$\sigma@HF = \frac{1}{(1+\beta)}\frac{S_H}{K_t \sqrt[m_H]{V}} \tag{9}$$

where S_L and S_H are the reference strength of the LS and HS materials, α and β are the modulus and thickness ratios of the LS to HS fibre layers, G_{IIC} is the mode II interlaminar fracture toughness of the interface between LS layers and HS layers of the hybrid composite, E_H the elastic modulus of the HS fibres, m_H is the Weibull strength distribution modulus of the HS fibre, S_H is the reference strength of the HS material, K_t is the stress concentration factor in the high strain material and V is the volume of the specimen (free length × width × total fibre layer thickness).

Hybrid configurations in which fragmentation in the LS material initiates before delamination should satisfy the $\sigma@LF < \sigma@del$ condition, resulting after some simplifications in the following inequality:

$$t_L < \frac{2G_{IIC}E_H}{{S_L}^2}\frac{\alpha(1-\gamma)}{(\alpha\gamma+1-\gamma)} \tag{10}$$

where γ is defined as:

$$\gamma = \frac{t_L}{t_L+t_H} = \frac{\beta}{1+\beta} \tag{11}$$

Hybrid configurations in which LS material fragmentation takes place before failure in the HS material should satisfy $\sigma@LF < \sigma@HF$ condition, resulting after some simplifications in the following inequality:

$$\sqrt[m]{t_L} < \frac{S_H}{K_t S_L}\left(\frac{\alpha}{\alpha\beta+1}\right)^{m_H}\sqrt{\frac{\beta}{2WL}} \quad (12)$$

where W is the width and L is the free length of specimens.

Hybrid configurations in which the HS material delamination stress failure stress, $\sigma@HF > \sigma@del$, delamination propagation is expected before final failure, satisfying the next inequality:

$$t_L^{\left(\frac{1}{2}-\frac{1}{m_H}\right)} > \beta^{-\frac{1}{m_H}}\frac{K_t}{S_H}\sqrt[m_H]{2WL}\sqrt{2G_{IIC}E_H}\sqrt{\frac{1+\alpha\beta}{\alpha}} \quad (13)$$

In all last models, S_L is assumed as a constant mean value, not taking into account the hybrid effect variation as function of the vol% of LS fibres, which would greatly contribute to 'yield' stress and pseudo-ductile strain of hybrid composites. In the present work, an actual strength of the LS material, $S_{L,a}$, was considered assuming the hybrid effect (computed according the PDM described in model description section).

$$S_{L,a} = S_L + (S_L \times fHE(V_L \times 100)) \quad (14)$$

where fHE is the hybrid effect a function of vol% of LS fibres.

DMMs were used to analyse the evolution and to identify the trade-offs between different responses in all damages modes, namely hybrid effect, 'yield' stress, pseudo-ductile strain, strength and elastic modulus. All the responses, with the exception of the elastic modulus (E_{hybrid}), were predicted with model of Jalalvand *et al.* [13], taking into account the equation (14). E_{hybrid} was predicted according to the rule of mixtures (see equation (15)) that has been proven to accurately estimate this property [6].

$$E_{hybrid} = V_L E_L + V_H E_H + V_M E_M \quad (15)$$

where V_L, V_H, V_M, E_L, E_H, and E_M are the volume and elastic modulus of the LS fibre, HS fibre and matrix, respectively.

In the present work, the mechanical properties experimentally characterized of UD non-hybrid composites were used as input variables of model (15) (see **Table 1**). The exact volume of resin was not directly controlled during the manufacturing. Cross-sectional area of the composite was computed considering only the thickness of the dry fabrics, according to the usual practice of the hand lay-up method [25]. In this way, E_L and E_H were considered the elastic modulus of LS and HS one layer composites, respectively. Therefore, the contribution of $V_M E_M$ was contemplated in $V_L E_L$ and $V_H E_H$ terms, leading to $V_L + V_H = 1$ and $V_M E_M = 0$.

Experimental procedure

Materials

Commercial dry UD fabrics available for civil engineering applications, with a similar areal mass of 400 g/m^2, were used in this work, namely UD HM carbon (S&P C-Sheet 640), ST carbon (S&P C-Sheet 240), E-glass (S&P G-sheet E 90/10) and basalt (Dalla Betta Group U400B-40-50-03). An epoxy-based material (S&P Resin Epoxy 55) was used as matrix for laminating the studied composites. According to the supplier, this epoxy has the following main properties [34]: (i) a tensile strength of 35.8 MPa; (ii) a strain at the failure of 2.3%; and, (iii) an elastic modulus of 2.6 GPa.

In **Table 1** the density, areal mass, and fibre layer thickness (areal mass density divided by the volumetric mass density) of UD fabrics are presented.

Tensile single fibre test

For each dry fabric, a reasonable number of single fibres (see **Table 1**) were randomly taken from the dry fabrics and tested. The method used follows the guidelines laid down in ASTM D3379-75 [31] for the

tensile testing of fibres. The measurements were performed in a Hounsfield H100KS universal testing machine with a load cell with 2.5 N maximum capacity (with an accuracy of ± 0.2% of applied force across load cell force range). In total, 200 fibres were individually mounted in the jig by means of a paper template with a fixed gauge length of 20 mm, see **Figure 3**. Fibre ends were bonded to the paper template by an ethyl cyanoacrylate-based adhesive. Then the tab ends were gripped in the jaws of the machine. Before the tensile tests were started, the paper template was cut across, so that just the fibre was fixed as a continuous length within the jig. The measurements were performed at a rate of 1.5 mm/min, until breakage occurred. For each fibre, records of applied load against extension were taken, and using an average mean diameter, determined through the analysis of microscopy images of fibres obtained with Scanning Electron Microscopy (SEM) (see **Figure 4**), the data registered were converted to stress-strain relationship.

In **Table 1** it is possible to observe that elastic modulus of single fibres is lower than the elastic modulus of cured composites. This is due to the fact that, in case of composites, the tensile properties were evaluated ignoring the contribution of the resin. This means that tensile strength was computed considering only the dry fabric thickness, which conducted to overestimation of the tensile strength and, consequently, large elastic modulus.

Hybrid composites

Hybrid composite of HM carbon/glass, ST carbon/glass, HM carbon/basalt, ST carbon/basalt and HM carbon/ST carbon up to 5 layers were studied. As resumed at **Table 3**, 16 series of hybrid composites results were compared with PDM predictions: 12 combinations with 3 reinforcing material layers and 6 combinations with 5 reinforcing material layers. The combinations of 3 symmetrical layers allowed to analyse the following approximate levels of LS fibre vol%: 0%, 33%, 66% and 100%. In addition, combinations with 5 layers allowed to analyse the following approximate levels of LS fibre vol%: 20%, 40% and 60%. Specimens with 5 layers were only tested on 2 hybrid combinations: HM carbon/glass and ST carbon/glass. Since each series was composed of 4 specimens, a total of 64 tests was carried out. It should be noted that the UD fabrics had slightly different thicknesses and, for this reason, the vol% before mentioned were corrected in the next sections, according to the corresponding thickness layer, assuming that vol% = $t_L/(t_L + t_H) \times 100$.

The hybrid composite laminates were manufactured by hand lay-up method, according to the best practices suggested in the guidelines [25], following this protocol: (i) dry fabrics were cut into pieces with 250 mm at parallel direction of fibres and 80 mm at perpendicular direction of fibres; (ii) a layer of epoxy was applied over a teflon film and in the first fabric layer with a brush; (iii) the fabric layer was adjusted manually, and then a ribbed rigid roller was used to apply pressure, in order to force excess resin and air out of the composite; (iv) the above mentioned steps were repeated for further layers. The top of the laminate was left rough, in order to simulate real applications. All the samples were then cured at room temperature (20 ± 0.5ºC) for 40 days.

Tensile tests

The specimens of each series were obtained from the laminates using a diamond tipped wheel cutter. Tensile tests were performed according to ISO 527-5:2009 standard [35]. Specimen dimensions were 250/150/15/[2.1-3.5]/[0.5-1.0] mm overall length/free length/width/total thickness/fibre layer thickness, respectively. Aluminium tabs of 50 × 15 mm^2 were used at each end of the specimen to avoid gripping effects. A clip gauge with a gauge length of 100 mm (with a linear error, including hysteresis of 0.25%) was used.

Tensile tests were carried out at room temperature on a universal testing machine (UTM) equipped with a 200 kN load cell (with a linear error less than 0.05% of full scale) and hydraulic grips. The specimens were held between grips of the UTM and extended (at a rate of 1 mm/min) up to failure.

As stated before, cross-sectional area of the composite was computed considering only the thickness of

the dry fabrics, according the recommendation suggested in the guidelines [25]. In this way, mechanical properties of impregnated composite (elastic modulus and tensile stress) were computed considering the wet lay-up system similar to an equivalent system of only dry fabrics. However, all the composites were measured with a digital calliper, which allowed to determine a fibre mean volume (Vf) of 23.4%, taking into account the fibre layer thickness reported by the manufacturer.

Results and discussion

Single fibre strength distributions

The strength distribution obtained by testing single fibres in tension is shown in **Figure 5** together with the Weibull model plotted by solid lines, considering L_0=20 mm and L=150 mm. The MLM was used to determine the Weibull parameters (shape and scale). The followed procedure is based in application of fitdist function available in Mathworks' Matlab R2015b [36]. The failure probabilities were estimated using the equation (16) (which is often used in the literature, e.g. [29, 32]) in order to allow the visualisation of the data, although it was not used to compute the distribution parameters, because MLM does not use such estimators [32].

$$P = \frac{i-0.3}{n+0.4} \tag{16}$$

where i is the i-th number in ascendingly ordered strength data and n is the sample size.

Visual examination of the diagrams indicates that the experimental data are reasonably well approximated by the chosen model. However, in the case of ST carbon fibres (**Figure 5** (c)) there was some discrepancy between experimental results and fitted model. As it was shown (in **Figure 4**), this type of fibres present the lowest diameter and for this reason they are more sensible to large stress deviations. It should be noticed that all stress results were computed considering an mean fibre cross-sectional area for converting load into stress.

The overall adequacy of the Weibull distribution was evaluated according to the chi-square goodness-of-fit test. This test depends on the number and the size of the classes of equal probabilities in which the data are grouped. For this reason, this approach maintains a certain degree of arbitrariness. The test result can be reported through the *p*-value approach [37] to state that the null hypothesis (described below) was or was not rejected at a specified level of significance. *P*-value varies between 0 and 1 and it is the smallest level of significance that would lead to rejection of the null hypothesis. In its turn, the level of significance is the probability wrongly reject the null hypothesis when it is true. For example a *p*-value lower or equal to 0.01 leads to the rejection of the null hypothesis with significant level of 1%.

The null hypothesis is defined as: the strength follows a Weibull distribution. The obtained *p*-values for the series tested are summarized in **Table 2**. It is possible to observe that all of the *p*-values for these goodness-of-fit statistics are larger than 0.01, implying that the null hypothesis cannot be reject with significant level >1%. The *p*-value obtained in basalt and E-glass cases is clearly superior to the obtained with the 2 types of carbon. Relatively to the ST carbon, the low *p*-value indicates the worst agreement of the experimental results with the Weibull distribution. However, the obtained *p*-value is high enough to avoid the rejection of null hypothesis. For this reason, the obtained parameters for the Weibull distributions were all accepted.

During the preparation of tests, mainly during the extraction of fibres, it was impossible to prevent some fibres from breaking, particularly the HM carbon ones. This is understandable, since the mean breaking force of all fibre types was very low, varying between 0.2 and 0.5 N. The elimination of the weakest fibres causes deviations from Weibull distribution and underestimates the scatter of strength (which means higher values of m). The m value of HM carbon is higher than in other cases. The experience gained in the execution of tests lead the authors of this work to believe that this value is not correct, since it was not possible to test a large number of weak fibres. As it is evident in tensile strength and hybrid effect predictions of hybrid composites section, assuming an m value equal to the mean of the 3 other types of fibres, i.e., m=2.70 lead to much better adjustment of the hybrid effect predictions. An algorithm that changes σ_0 of CHM fibres while maintaining either the same strength was implemented,

this means that failure strain of CHM was changed. The parameters that define this hypothetical distribution are as well exposed in **Table 2**.

Tensile strength and hybrid effect predictions of hybrid composites

The variation of vol% of LS fibres greatly modify the hybrid tensile response. The PDM, equation (6), is obviously sensitive to this variation. An example of the evolution of the stress–strain analytical relationships of the CHM/G combination as the vol% of LS fibres increases are plotted in **Error! Reference source not found.**. It is possible to observe that when the vol% of HM carbon fibres increases, the strength of the hybrid composite is no longer dominated by glass fibres and depends on the contribution of the two types of fibres. This behaviour essentially follows the bilinear rule of mixtures (ROM):

$$\sigma_{hybrid} = \begin{cases} V_L S_L + V_H E_H \varepsilon_L;\ V_H < V_{crit} \\ V_H S_H;\ V_H > V_{crit} \end{cases} \quad (17)$$

where σ_{hybrid} is tensile strength of hybrid composites and ε_L is the ultimate strain of the LS composite. Based on this model, if the V_H is lower than a critical value, $V_{crit,}$ the hybrid composite would fail prematurely. On the other hand, if the V_H is higher than V_{crit}, hybrid composites would keep their integrity until the failure of HS fibre.

As shown in **Figure 6**, the strength predictions follow completely the bilinear ROM. The input parameters used to define the bilinear ROM derived from PDM model: the reference HM carbon composite has a strength of 1350 MPa, an elastic modulus of 100.0 GPa and a failure strain of 1.35%, while the reference glass composite has a strength of 2080 MPa, an elastic modulus of 13.6 GPa and a failure strain of 15.24%. V_{crit} was calculated by equating the two branches of equation (17) and it was determined equal to 41.6%. The predicted failure strains of the composites exceed a lot the experimental values (see **Table 1**), which lead to very low values of elastic modulus. In this way, the PDM cannot be considered a good model to predict the failure strains. Swolfs *et al.* [9] obtained the same conclusion and they believe that this is due to the fact the GLS models neglect the stress concentrations. In the work of Turon *et al.* [19], it was referred that failure prediction is out of the scope of the present model.

The two different sets of Weibull parameters were used as inputs of PDM in CHM fibres case: (i) the m=5.51 and σ_0= 4559.57 MPa, pair computed according to the experimental tensile CHM fibres strength distribution, and (ii) the m=2.70 and σ_0=2874.00 MPa pair, hypothetical suggested. It is possible to observe in Figure 6 and Figure 7 that the suggested change had no impact in the strength predictions, but had a great influence in the hybrid effect predictions, improving reasonably the predictions of this property.

In **Figure 7** the mean (and the 95% Fisher level of confidence intervals) of hybrid effect are compared against the PDM predictions. As it is shown, the predictions are, in general, in good agreement with the obtained experimental results. Quantitative comparisons between analytical and experimental results are presented in **Table 3**.

It can be seen that apparently very high relative errors (between -251.7% and 2597.5%) were registered. However, it is possible to observe that very high relative errors were registered in cases in which experimental hybrid effects were negative. Experimental negative hybrid effects only make sense because the number of layers of LS material is not the same in all hybrid combinations. It is well-known that there is a size effect in tensile properties of reinforcing fibre due to the higher probability of finding a cluster of weaker fibre in a larger volume of material [8]. In cases where the hybrid effect was negative, 2 or 3 layers of LS fibre were used. Since the hybrid effect was computed relatively to the 1 layer non-hybrid composite results, negative hybrid effects are understandable. The influence of size effect on the hybrid effect has not yet been investigated in the literature [8]. In any case, in combinations in which the hybrid effect was negative, the predictions are very close to zero, which would be a plausible prediction if the size effect did not exist. With the exception of 2 combinations (1G/1CHM/1G/1CHM/1G and 2G/1C/2G), the positive hybrid effects were predicted satisfactorily, with relative errors varying between -20.4% and 31.1%.

Analytical hybrid effects were used to computed $S_{L,a}$ (according to equation (14)). The results are

exposed in **Table 3**. It is possible to observe that $S_{L,a}$ was predicted satisfactorily, with relative errors varying between -25.4% and 14.7%

In view of the above, PDM is a simple model that, if used with care, can predict reasonably the hybrid effect. However, some limitations should be considered, for instances: (i) it does not take into account the real number of fibres, leading to size effects being ignored. Furthermore, (ii) it ignores the dispersion of fibres, which has been shown to be a very important parameter affecting the hybrid effect [38].

Damage mode maps

In this section, the influence of the geometric and reinforcing material combinations in different characteristics of the hybrid stress–strain response, such as hybrid effect, 'yield' stress, pseudo-ductile strain, strength and elastic modulus of the hybrid composites is investigated. The main objective of this part of the work is to better understand the potential of the hybridization of the studied materials, and to identify which combinations maximize the tensile response.

Hybrid effect

The evolution of the hybrid effect for the different reinforcing material combinations is presented in **Figure 8**. The presentation of the results for hybrid effect is based on DMMs described in Evolution of hybrid properties (damage mode maps) section.. Each DMM locates four zones that divide all possible expected tensile damage modes of UD hybrid composites. The horizontal axis of DMMs shows the ratio between LS and HS material thickness and the vertical axis shows the absolute thickness of LS material. The border lines are defined for each material combination according to the equations (10), (12) and (13). In innovative way, the evolution of S_L was contemplated according the predictions of hybrid effect, assuming $S_L = S_{L,a}$. This means that mean values presented in the **Table 1** and the corresponding computed hybrid effect were updated as function of the ratio between the thicknesses of the reinforcing materials. This option had influence in the definition of the boundaries that depend on S_L, namely those which are defined in equations (10) and (12) .The length and width of specimens were assumed equal to L = 150 mm and W = 15 mm, respectively. The interlaminar toughness, G_{IIC}, for the different hybrid interfaces was not experimentally measured and it was arbitrated in way that, in combination with experimental pseudo-ductile behaviour, the fragmentation & dispersed delamination damage mode was analytically achieved (see the details in [6]). Weibull modulus of HS fibres was assumed constant and equal to the value used by Jalalvand *et al.* [13], m_H = 29.3. This value is significantly higher than that obtained experimentally in this work (and higher than those usually reported in bibliography, e.g. [27]). However, it was proved by the authors' model [13] that this value allowed the best predictions. In practice, this implies that a lower variability of HS fibres strength is being considered. The value of 0.97 means that strength of HS fibres is higher in hybrids than non-hybrid composites. This could means that there is not stress concentration at HS fibres of hybrids or that stress concentration has influence the non-hybrid results. This subject should be further explored.

In general terms, observing the **Figure 8**, it is possible to conclude that the combination of HM carbon with ST carbon allowed to achieve the maximum hybrid effect (at least close to 50%). For all the combinations the maximum hybrid effect was achieved with the occurrence of fragmentation or fragmentation & delamination.

In **Figure 9** the DMMs of different reinforcing material combinations are presented in conjugation with the localization of experimental configurations and indication of vol% of LS fibres. The border lines defined with the contemplation of a mean experimental $S_{L,a}$ and analytical $S_{L,a}$ are compared. The mean experimental $S_{L,a}$ was computed assuming the mean value obtained for all series within the material combination. It is possible to observe that the contemplation of analytical $S_{L,a}$ reduced the fragmentation and fragmentation & delamination zones. In this way, the premature failure and catastrophic delamination damages modes occur much more frequently. Anyway, in both cases the boundaries in **Figure 9** separate the studied configuration in absolute accordance with registered damage modes exposed in [6]. However, in the case of HM carbon/glass combination, the configuration with 38.2% of LS fibres is located very close to the border line. This point is even slightly outside of fragmentation &

delamination zone, considering boundaries with analytical $S_{L,a}$ contemplation. In this case, the $S_{L,a}$ are a little overestimated. In the remaining cases, all the points that correspond to combinations in which the pseudo-ductile was achieved are located in fragmentation and stable delamination zone. This happened essentially with some combinations that included HM carbon as the LS material. For other hand, configuration in which the ST carbon is considered the LS material, it is possible to observe that the fragmentation and fragmentation & delamination zones are very reduced, indicating that it is almost impossible to get these types of damage modes in practice. For instance, the abscissa point of the apex of the boundary lines of ST carbon/glass combination is 0.1548. A layer of ST carbon has a thickness of 0.223 mm (see **Table 1**), this means that in the referred point the thickness of the glass is 1.505 mm, which corresponds approximately to 9.77 layers. The best practices suggested in the guidelines [25] advise to use no more than 5 layers.

'Yield' stress and pseudo-ductile strain

DMMs presented in **Figure 10** allow to observe that the highest value of 'yield' stress, if it exists, can be achieved close to LS fragmentation/HS failure boundary. This means that this property increases with the amount of the LS fibres. 'Yield' stress was computed for all the combinations according to equation (7). S_L was assumed equal to analytical $S_{L,a}$. The maximum 'yield' stress was achieved for the combination of ST carbon with basalt. However, in this material combination, the reduced areas of the fragmentation and fragmentation & delamination zones leads almost to the impossibly of achieving this damage mode in practice. In this way, the combination of HM carbon with ST carbon is the best plausible choice to reach the highest 'yield' stress.

The predicted pseudo-ductile strains for all material combinations are present in **Figure 11**. As in the previous case, the coloured regions of the maps indicate the existence of pseudo-ductility. The white regions show either premature HS material failure or catastrophic delamination. It is possible to observe that the highest value of pseudo-ductile strain can be achieved close to the intersection of the boundaries within fragmentation & delamination zones. This is understandable because delamination promotes extra extension to the composite, when compared to the case in which only fragmentation takes place. The highest values of pseudo-ductile were achieved in the combination of HM carbon with basalt. On the other hand, the combination of HM carbon with ST carbon resulted in the worst response. Again, the pseudo-ductile strain in the combination of ST carbon with glass or basalt are very difficult to achieve experimentally. The predicted pseudo-ductile strains are presented in **Table 3** and they are compared with experimental results. Although, the relative errors are very high, absolute values are close. Comparing very low values generates situations where small variations lead to very high relative errors. For this reason, this type of errors should be carefully analysed.

Strength and elastic modulus

The strength was predicted according to the equations (7) and (8). For each configuration, the maximum between $\sigma@LF$ and $\sigma@HF$ was assumed as the strength. The evolution of the strength for studied hybrid combinations is presented in **Figure 12**. It is possible to observe that, in all cases, the minimum strength was achieved in LS fragmentation/delamination boundary. The evolution of strength follows basically the conclusions obtained with bilinear ROM. The highest strength was achieved with the combination of ST carbon with basalt. Since HM carbon is one of the materials with lower tensile strength, in combination with this material, the increase of volume of HM carbon would not lead to significant improvements in tensile strength. Experimental and analytical strengths are presented in **Table 3**. It is possible to observe that strength was reasonably predicted, with relative errors varying between -36.1% and 26.1%.

Figure 13 presents the evolution of elastic modulus of the 5 material combinations referred before. This property was evaluated according to equation (15). As expected, the elasticity modulus increases with the thickness increase of LS fibres in all the combinations. It is possible to observe that the property under review varies only with thickness ratio between the reinforcing materials, i.e. the absolute LS layer thickness has no influence in the response. Combinations that include HM carbon are the ones that allow reaching higher elasticity modulus. According to the DMMs shown in **Figure 13**, the combination of HM carbon with ST carbon results in the highest elastic modulus and the combination of carbon with

glass in the lowest values.

Conclusions

In the present work, it was concluded that PDM, if used with care, can predict reasonably the hybrid effect. However, there are some limitations, because the method does not take into account scale effects or the dispersion of fibres. Furthermore, Weibull parameters, which are used as inputs of the PDM, are susceptible to several error sources and they are dependent of the number of tests and the gauge length of specimens. Having said that, quantitative comparisons between analytical and experimental revealed that positive hybrid effects were predicted with relative errors varying between -20.4% and 31.1%. It was explained that negative hybrid effects appear probably due to the size effect in tensile properties of reinforcing fibre due to the higher probability of finding a cluster of weaker fibre in a larger volume of material. It should be highlighted that it is not possible, in combination with low vol% of LS fibres, to achieve a clear local maximum point at stress-strain diagram predicted with PDM, corresponding to strain to failure of LS fibres. In these cases, the hybrid effect was considered equal to the achieved with lowest possible vol% of LS fibres.

Analytical hybrid effects were used to compute the reference strength of LS fibres and it was demonstrated that this property was reasonably predicted, with relative errors varying between -25.4% and 14.7%. Furthermore, analytical hybrid effects were considered to modify the model of Jalalvand et al. [13] and, in this way, to predict pseudo-ductile strain and strength. It was demonstrated that the magnitude of the two cited properties is close to the experimental results.

DMMs of different reinforcing material combinations were presented. The border lines were defined with the contemplation of the hybrid effect. It was possible to observe that this contemplation reduced the fragmentation and fragmentation & delamination zones. DMMs allowed as well to observe that the highest value of 'yield' stress can be achieved if the coordinates of a given hybrid configuration are close to LS fragmentation\HS failure boundary. In configurations where the ST carbon was considered as the LS material, it was possible to observe that the fragmentation and fragmentation & delamination zones were very reduced, indicating that it is almost impossible to get these types of damage modes in practice. In this way, the combination of HM carbon with ST carbon is the best plausible choice to reach the highest 'yield' stress.

It was also possible to observe that the highest value of pseudo-ductile strain can be achieved close to the intersection of the boundaries within fragmentation & delamination zone. The highest values of pseudo-ductile were achieved in the combination of HM carbon with basalt.

It was also possible to observe that in all cases the minimum strength was achieved in LS fragmentation/ delamination boundary. The highest strength was achieved with the combination of ST carbon with basalt.

As expected, the elasticity modulus increases with the increase of thickness of LS fibres in all the combinations. The combination of HM carbon with ST carbon resulted in the highest elastic modulus.

Acknowledgments

The first author wish to thank to FCT - Portuguese Foundation for Science and Technology and to the Doctoral Program Eco-Construction and Rehabilitation for supporting the PhD scholarship (with the reference PD/BD/52660/2014). The second author acknowledge the grant SFRH/BSAB/150266/2019 provided by FCT, financed by European Social Fund and by national funds through the FCT/MCTES. This work is part of the research project ''EasyFloor – Development of composite sandwich panels for rehabilitation of floor buildings", involving the company ALTO – Perfis Pultrudidos, Lda., CERis/Instituto Superior Técnico and ISISE/University of Minho, supported by FEDER funds through the Operational Program for Operational Program for Competitiveness and Internationalization (POCI) and the Portuguese

National Innovation Agency (ANI) – project no. 340 (POCI-01-0247-FEDER-003480). Acknowledgments are extended to LEST – Laboratório de Estruturas for their material support. Finally, the authors also like to thank to the company S&P Clever Reinforcement Ibérica Lda and Dalla Betta Group Company for the material provided.

REFERENCES

1. Czél G, Jalalvand M, Wisnom MR and Czigány T. Design and characterisation of high performance, pseudo-ductile all-carbon/epoxy unidirectional hybrid composites. *Composites Part B*. 2017; 111 348-356.
2. Czél G, Jalalvand M and Wisnom MR. Design and characterisation of advanced pseudo-ductile unidirectional thin-ply carbon/epoxy–glass/epoxy hybrid composites. *Composite Structures*. 2016; 143: 362–370.
3. Summerscales J and Short D. Carbon fibre and glass fibre hybrid reinforced plastics. *Composites*. 1978; 9: 157–166.
4. Czél G and Wisnom MR. Demonstration of pseudo-ductility in high performance glass/epoxy composites by hybridisation with thin-ply carbon prepreg. *Composites: Part A: Applied Science and Manufacturing*. 2013; 52: 23–30.
5. Swolfs Y, Gorbatikh L and Verpoest I. Fibre hybridisation in polymer composites: a review. *Composites Part A: Applied Science and Manufacturing*. 2014; 67: 181-200.
6. Ribeiro F, Sena-Cruz J, Branco FG and Júlio E. Hybrid effect and pseudo-ductile behaviour of unidirectional interlayer hybrid FRP composites for civil engineering applications. *Construction and Building Materials*. 2018; 171: 871-890.
7. Hayashi T. On the improvement of mechanical properties of composites by hybrid composition. *Proc 8th Intl Reinforced Plastics Conference*. 1972: 149-152.
8. Wisnom MR, Czél G, Swolfs Y, Jalalvand M, Gorbatikh L and Verpoest I. Hybrid effects in thin ply carbon/glass unidirectional laminates: Accurate experimental determination and prediction. *Composites: Part A*. 2016; 88: 131–139.
9. Swolfs Y, McMeeking RM, Rajan VP, Zok FW, Verpoest I and Gorbatikh L. Global load-sharing model for unidirectional hybrid fibre-reinforced composites. *Journal of the Mechanics and Physics of Solids*. 2015; 84: 380–394.
10. Swolfs Y, Gorbatikh L and Verpoest I. Stress concentrations in hybrid unidirectional fibre-reinforced composites with random fibre packings. *Composites Science and Technology*. 2013; 85: 10–16.
11. Zweben C. Tensile strength of hybrid composites. *Journal of Materials Science* 1977; 12: 1325-1337.
12. Fukuda H. An advanced theory of the strength of hybrid composites. . *Journal of Materials Science*. 1983; 19: 974-982.
13. Jalalvand M, Czél G and Wisnom MR. Damage analysis of pseudo-ductile thin-ply UD hybrid composites – A new analytical method. *Composites: Part A*. 2015; 69: 83–93.
14. Curtin WA. Theory of Mechanical Properties of Ceramic-Matrix Composites. *J Am Ceram Soc*. 1991; 74: 2837-2845
15. Curtin WA. Stochastic Damage Evolution and Failure in Fiber-Reinforced Composites. *Advances in Applied Mechanics Volume*. 1998; 36: 163-253.
16. Hui C-Y, Phoenix SL, Ibnabdeljalil M and Smiths RL. An exact closed form solution for fragmentation of Weibull fibers in a single filament composite with applications to fiberreinforced ceramics. *J Mech Phys Solids*. 1991; 43: 1551-1585.
17. Rajan VP and Curtin WA. Rational design of fiber-reinforced hybrid composites: A global load sharing analysis. *Composites Science and Technology* 2015; 117: 199-207.
18. Tavares RP, Melro AR, Bessa MA, Turon A, Liu WK and Camanho PP. Mechanics of hybrid polymer composites: analytical and computational study. *Comput Mech DOI 101007/s00466-015-1252-0*. 2016.
19. Turon A, Costa J, Maimí P, Trias D and Mayugo JA. A progressive damage model for unidirectional fibre-reinforced composites based on fibre fragmentation. Part I: Formulation. *Composites Science and Technology*. 2005; 65 2039–2048.
20. Pan N and Postle R. The tensile strength of hybrid fibre composites: a probabilist analysis of hybrid effects. *Phil Trans R Soc Lond A*. 1996; 354: 1875-1897.
21. Manders PW and Bader MG. The strength of hybrid glass/carbon fibre composites - Part 1. *Journal of Materials Science*. 1981; 16: 2233-2245.
22. Kretsis G. A review of the tensile, compress,ve, flexural and shear properties of hybrid fibre reinforced plastics. *Composites*. 1987; 18.

23. Shan Y and Liao K. Environmental fatigue behavior and life prediction of unidirectional glass–carbon/epoxy hybrid composites. *International Journal of Fatigue*. 2002; 24: 847–859.
24. Yu H, Longana ML, Jalalvand M, Wisnom MR and Potter KD. Pseudo-ductility in intermingled carbon/glass hybrid composites with highly aligned discontinuous fibres. *Composites: Part A* 2015; 73: 35–44.
25. CNR-DT200. Guide for the Design and Construction of Externally Bonded FRP Systems for Strengthening Existing Structures. Advisory Committee on Techincal Recommendations for Construction, National Research Council, Rome, Italy. 2013.
26. Jalalvand M, Czél G and Wisnom MR. Parametric study of failure mechanisms and optimal configurations of pseudo-ductile thin-ply UD hybrid composites. *Composites: Part A*. 2015; 74: 123–131.
27. Swolfs Y, Verpoest I and Gorbatikh L. A review of input data and modelling assumptions in longitudinal strength models for unidirectional fibre-reinforced composites. *Composite Structures*. 2016; 150: 153–172.
28. Weibull W. A Statistical Distribution Function of Wide Applicability. 1951: 293-297.
29. Andersons J, Joffe R, Hojo M and Ochiai S. Glass fibre strength distribution determined by common experimental methods. *Composites Science and Technology* 2002; 62: 131–145.
30. Swolfs Y, Verpoest I and Gorbatikh L. Issues in strength models for unidirectional fibre-reinforced composites related to Weibull distributions, fibre packings and boundary effects. *Composites Science and Technology* 2015; 114: 42–49.
31. ASTM. D 3379 – 75 - Standard Test Method for Tensile Strength and Young's Modulus for High-Modulus Single-Filament Materials. 1989.
32. Ambrožič M and Gorjan L. Reliability of a Weibull analysis using the maximum-likelihood method. *Journal of materials science*. 2011; 46: 1862-1869.
33. Fotouhi M, Suwarta P, Jalalvand M, Czel G and Wisnom MR. Detection of fibre fracture and ply fragmentation in thin-ply UD carbon/glass hybrid laminates using acoustic emission. *Composites: Part A* 2016; 86: 66–76.
34. S&P. Technical Data Sheet S&P Resin 55. 2015.
35. ISO. 527-5 Plastics — Determination of tensile properties; Part 5: Test conditions for unidirectional fibre-reinforced plastic composites. EUROPEAN COMMITTEE FOR STANDARDIZATION. 2009.
36. MATLAB Release 2015b, The MathWorks, Inc., Natick, Massachusetts, United States.
37. Montgomery DC and Runger GC. Applied Statistics and Probability for Engineers. *John Wiley & Sons, Inc ISBN-13 9781118539712*. 2014.
38. Swolfs Y, McMeeking RM, Verpoest I and Gorbatikh L. The effect of fibre dispersion on initial failure strain and cluster development in unidirectional carbon/glass hybrid composites. *Composites: Part A* 2015; 69: 279–287.

List of Tables

Table 1 — Properties of the dry fabrics, fibres and cured composite materials determined experimentally.

Material ID	Properties of the dry fabric, as reporter by the manufacturer			Properties of the fibres (tested according to ASTM D3379)					Properties of 1 ply composites [6]*		
	Density [g/m^3]	Areal mass [g/m^2]	Fibre layer thickness [mm/layer]	N. of samples	Fibre diameter [µm] (CoV [%])	Elastic modulus [GPa] (CoV [%])	Tensile strength [MPa] (CoV [%])	Strain at the failure [%] (CoV [%])	Elastic modulus [GPa] (CoV [%])	Tensile strength [MPa] (CoV [%])	Strain at the failure [%] (CoV [%])
Basalt (B)	2.67	420	0.157	50	18.14 (3.56)	61.41 (31.14)	1886.70 (40.79)	3.10 (27.73)	102.5 (15.46)	2244.2 (20.17)	2.46 (10.61)
E-glass (G)	2.60	400	0.154	50	14.98 (16.25)	76.92 (27.97)	2662.06 (33.88)	3.72 (20.45)	81.6 (7.39)	1671.2 (8.59)	2.31 (3.78)
ST carbon (C)	1.79	400	0.223	36	7.88 (5.15)	213.95 (43.36)	3920.67 (39.37)	1.38 (17.37)	231.3 (12.50)	2565.9 (10.18)	1.09 (8.81)
HM carbon (CHM)	2.10	400	0.190	26	11.03 (6.66)	558.07 (24.67)	2934.24 (19.16)	0.53 (18.99)	624.1 (11.13)	1749.4 (24.39)	0.27 (19.61)

Notes: *The tensile properties were computed considering only the thickness of the dry fabrics, according the recommendation suggested in the guidelines [31]. Elastic modulus is defined as the slope of stress-strain curve between the strains 0.0005 and 0.0025.

Table 2 — Weibull distribution parameters.

Material ID	L_0 [mm]	L [mm]	σ_0 [MPa]	m	p-value
B	20	150	4593.83	2.61	0.5496
G	20	150	5965.90	2.80	0.1455
C	20	150	9353.44	2.68	0.0267
CHM	20	150	4559.57	5.51	0.0547
(Hypothetical) CHM*	20	150	2874.00	2.70	--

Note: *m value was assumed equal to the mean of the 3 other types of fibres because the elimination of the weakest fibres underestimates the strength scatter.

Table 3 — Comparison between experimental and analytical results.

Combinations	Series ID	Volume of LS fibre [%]	Hybrid effect			$S_{L,a}$ [MPa]			Tensile streng			Pseudo-ductile strain		
			Experimental [%] [6]	PDM prediction [%]	Error [%]	Experimental [MPa] [6]	Based on predicted HE [MPa]	Error [%]	Experimental [MPa] [6]	Analytical [MPa]	Error [%]	Experimental [%] [6]	Analytical [%]	Error [%]
C/B	1C/1B/1C	74.0	-8.99	3.21	135.7[a]	2289.9	2648.3	-15.65	2191.4 (7.28)	2264.6	-3.3	--	--	--
	1B/1C/1B	41.5	17.37	11.97	31.1	2960.6	2873.0	2.96	1950.2 (7.51)	1938.2	0.6	--	--	--
CHM/B	1CHM/1B/1CHM	70.8	-12.95	1.44	111.2[a]	1497.8	1774.6	-18.48	1150.0 (14.10)	1341.0	-16.6	--	--	--
	1B/1CHM/1B	37.7	30.19	25.36	16.0	2246.8	2193.0	2.39	1328.0 (10.74)	1125.3	15.3	2.04 (8.84)	1.80	11.8
CHM/C	1CHM/1C/1CHM	63.0	-1.50	8.69	680.1[a]	1684.8	1901.4	-12.84	1352.5 (5.10)	1458.8	-7.9	--	--	--
	1C/1CHM/1C	29.5	44.52	40.58	8.9	2434.0	2459.3	-1.04	1937.5 (6.79)	1431.0	26.1	0.44 (9.57)	0.64	-45.5
C/G	1C/1G/1C	74.3	-4.44	3.85	186.6[a]	2405.0	2664.7	-10.77	2176.9 (8.55)	2222.0	-2.1	--	--	--

	1G/3C/1G	68.5	-0.20	5.13	2597.5[a]	2521.2	2697.5	-7.00	2216.0 (8.77)	2143.7	3.3	--	--	--
	1G/1C/1G/1C/1G	49.1	9.15	11.01	-20.4	2752.5	2848.4	-3.49	1776.3 (10.55)	1910.4	-7.5	--	--	--
	1G/1C/1G	42.0	16.33	14.22	12.9	2937.5	2930.8	0.23	1856.0 (5.67)	1830.6	1.3	--	--	--
	2G/1C/2G	26.6	7.33	25.77	-251.7	2706.2	3227.1	-19.25	1244.4 (1.74)	1693.6	-36.1	--	--	--
CHM/G	1CHM/1G/1CHM	71.2	-7.07	2.17	130.7[a]	1560.3	1787.4	-14.56	1168.9 (19.49)	1339.3	-14.6	--	--	--
	1G/3CHM/1G	64.9	-14.09	2.89	120.6[a]	1435.4	1800.0	-25.40	1053.5 (10.14)	1251.1	-18.8	--	--	--
	1G/1CHM/1G/1CHM/1G	45.1	27.66	6.52	76.4	2184.4	1863.5	14.69	1105.8 (9.18)	974.7	11.9	--	--	--
	1G/1CHM/1G	38.2	9.97	8.69	12.8	1872.0	1901.4	-1.56	1054.7 (9.11)	879.1	16.6	1.21 (23.32)	1.73	-43.0
	2G/1CHM/2G	23.6	21.94	19.57	10.8	2059.5	2091.8	-1.56	1164.7 (14.47)	1004.6	13.7	1.4 (15.20)	1.66	-18.6

Note: [a]apparently very high relative errors were registered in cases that hybrid effect was negative.

List of Figures

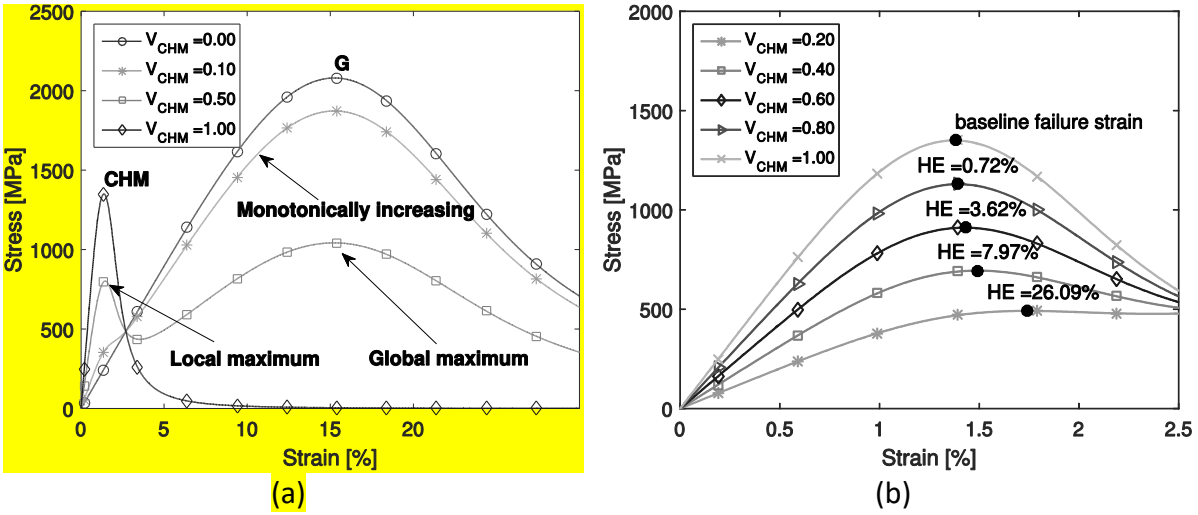

Figure 1 — PDM predictions: (a) identification of stress–strain curve with monotonic increase; (b) zoomed stress–strain curves of HM carbon/glass combination and identification of hybrid effect (HE).

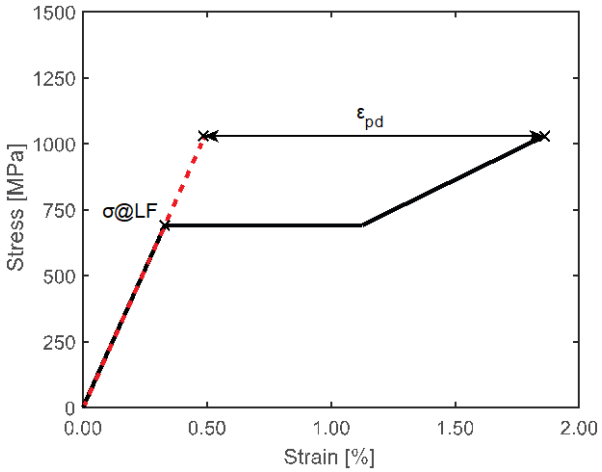

Figure 2 — Illustration of nonlinear pseudo-ductile behaviour and definitions of 'yield' stress and pseudo-ductile strain (adapted from [1]).

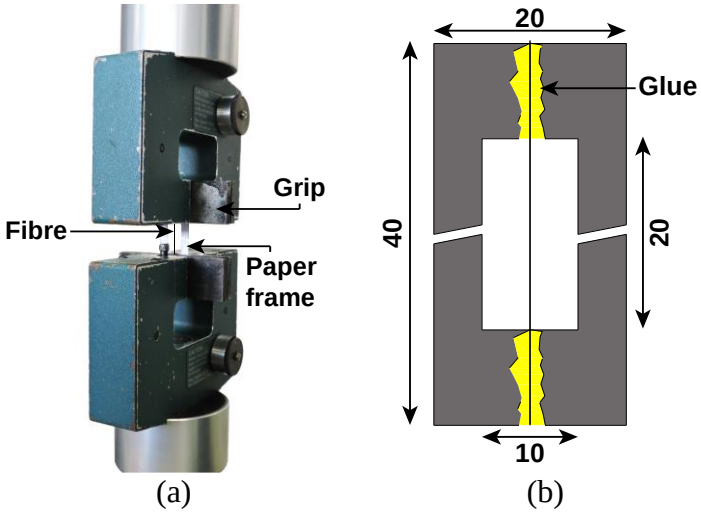

Figure 3 — Tensile fibre test: (a) illustration of the test and (b) geometry of specimen (dimensions in mm).

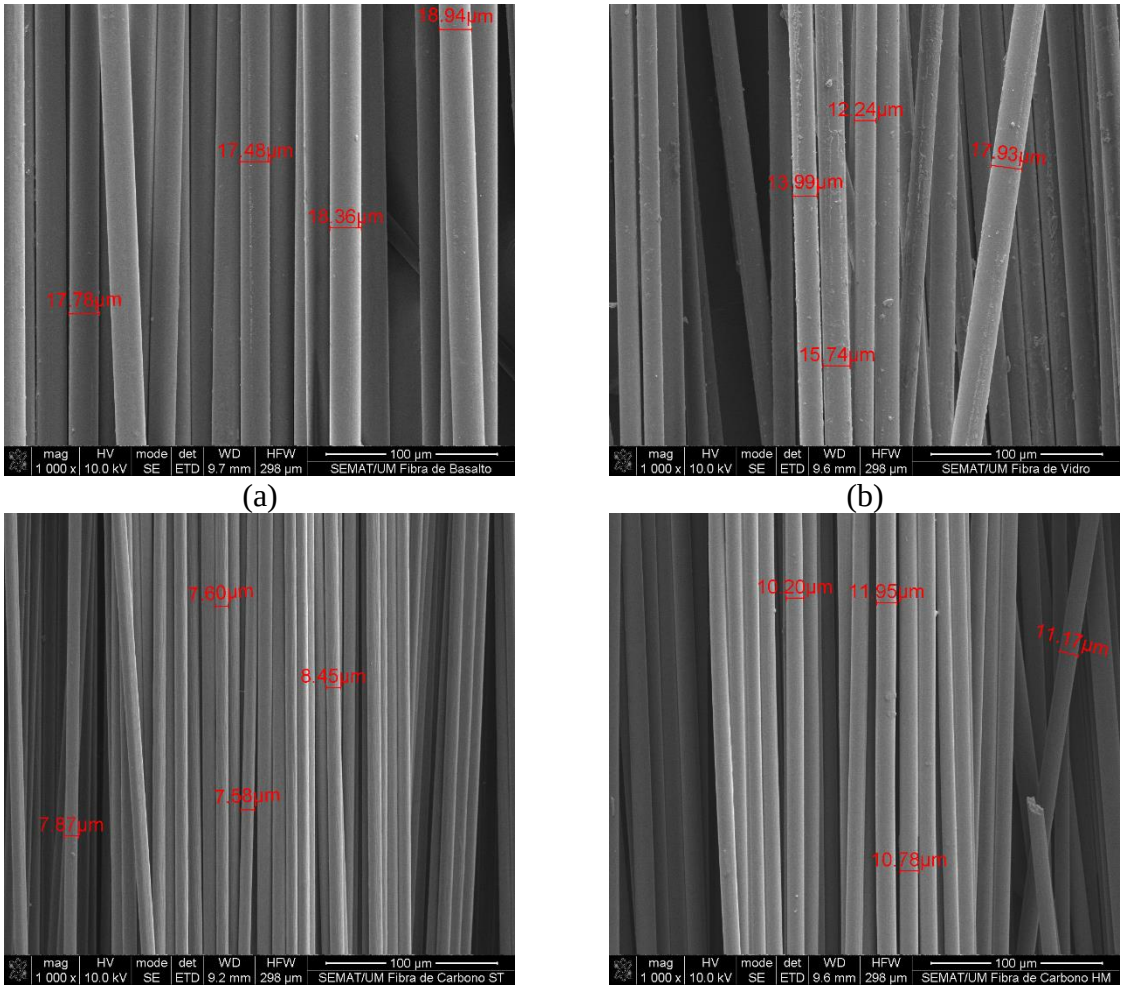

Figure 4 — SEM images of the surface and diameter indication of: (a) glass fibres; (b) basalt fibres; (c) ST carbon and (d) HM carbon.

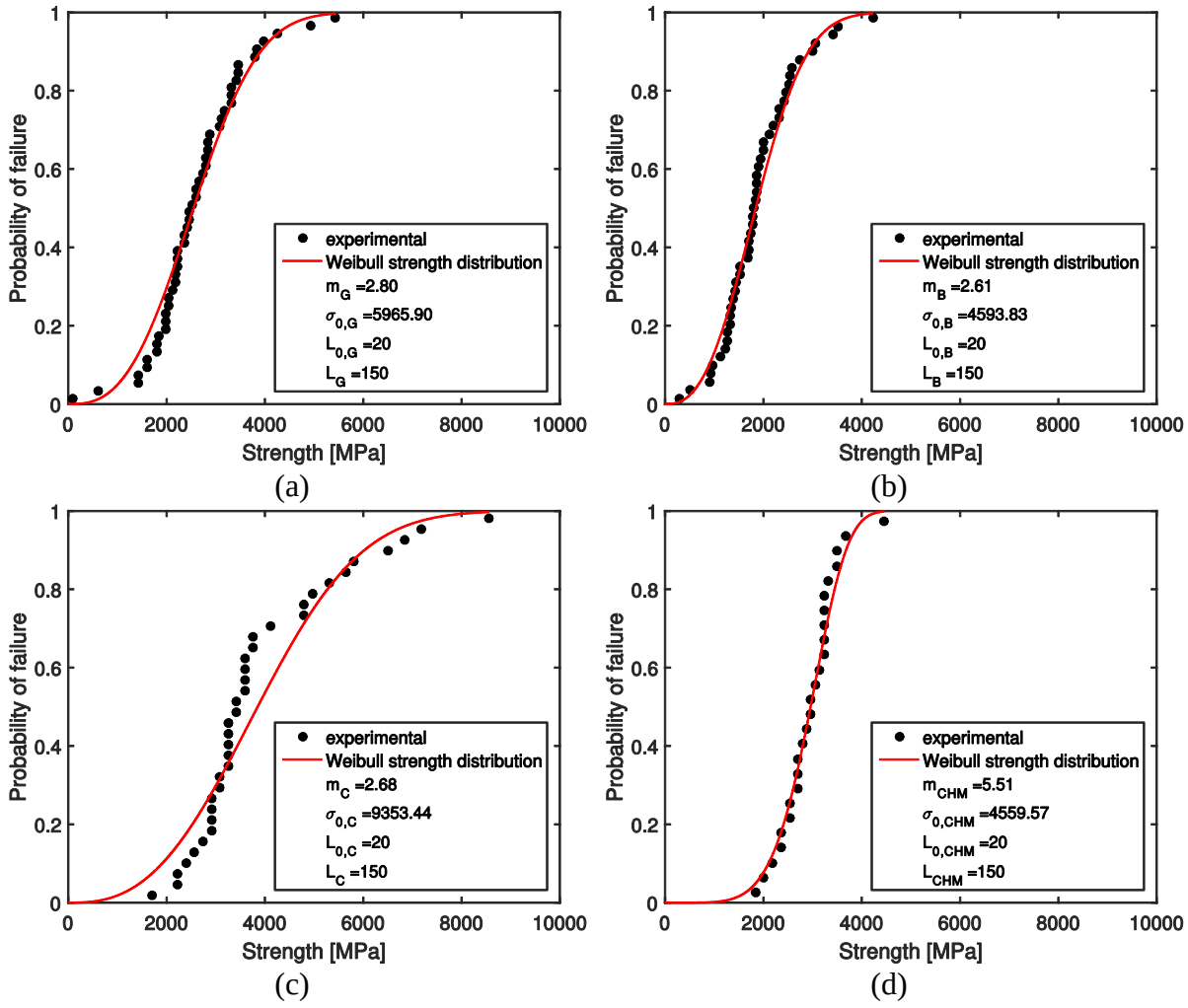

Figure 5 — Cumulative Weibull fibre strength distribution for: (a) glass fibres; (b) basalt fibres; (c) ST carbon; (d) HM carbon.

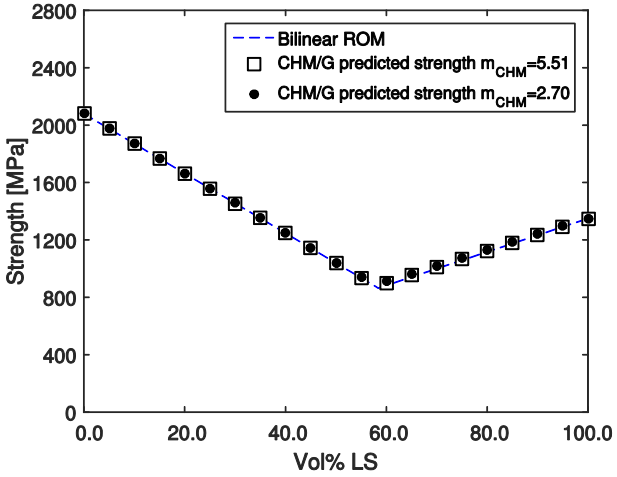

Figure 6 —PDM strength predictions compared with the bilinear rule-of-mixtures as function of Weibull modulus and relative volume of HM carbon fibres.

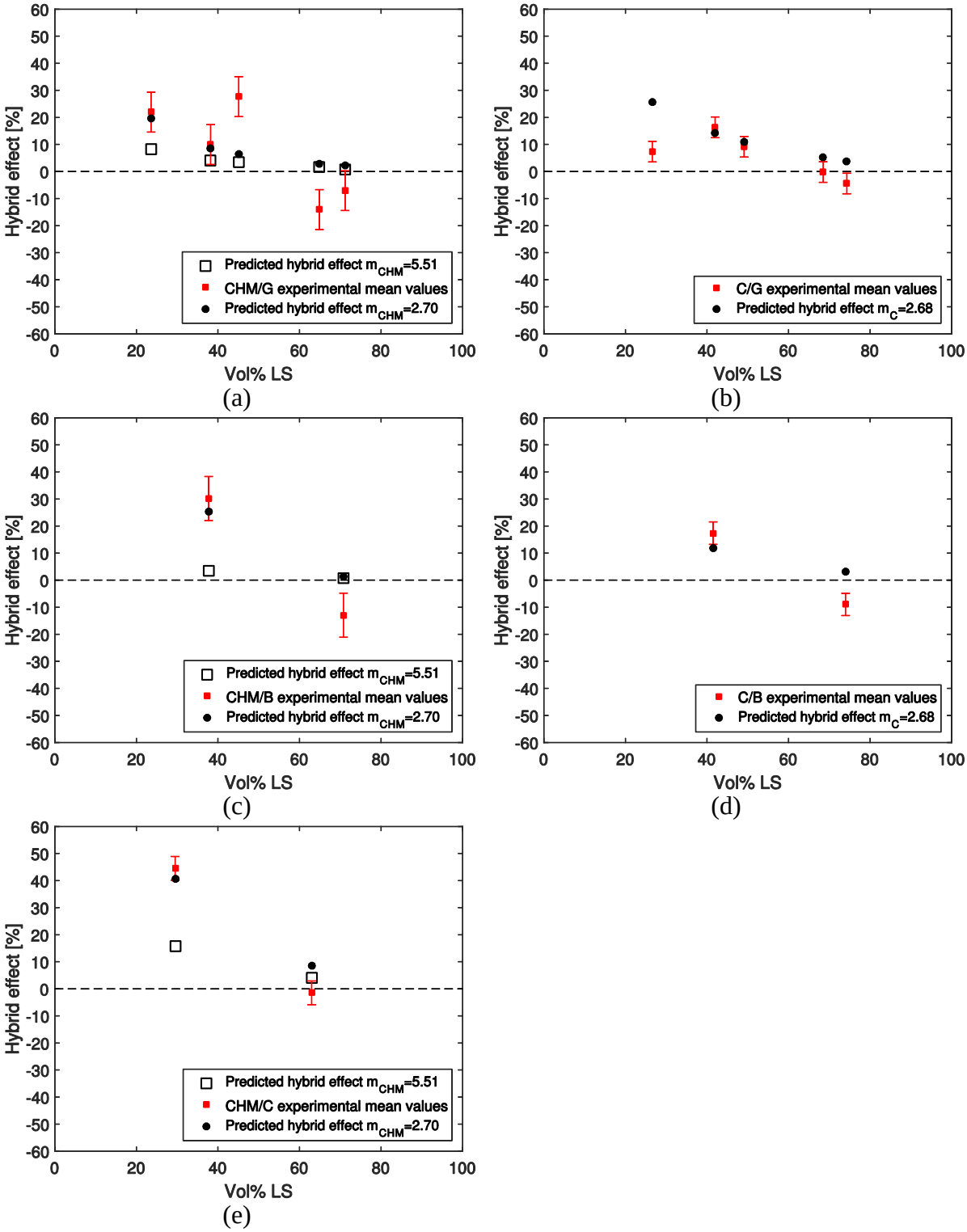

Figure 7 — Experimental mean hybrid effect results compared with analytical predictions.

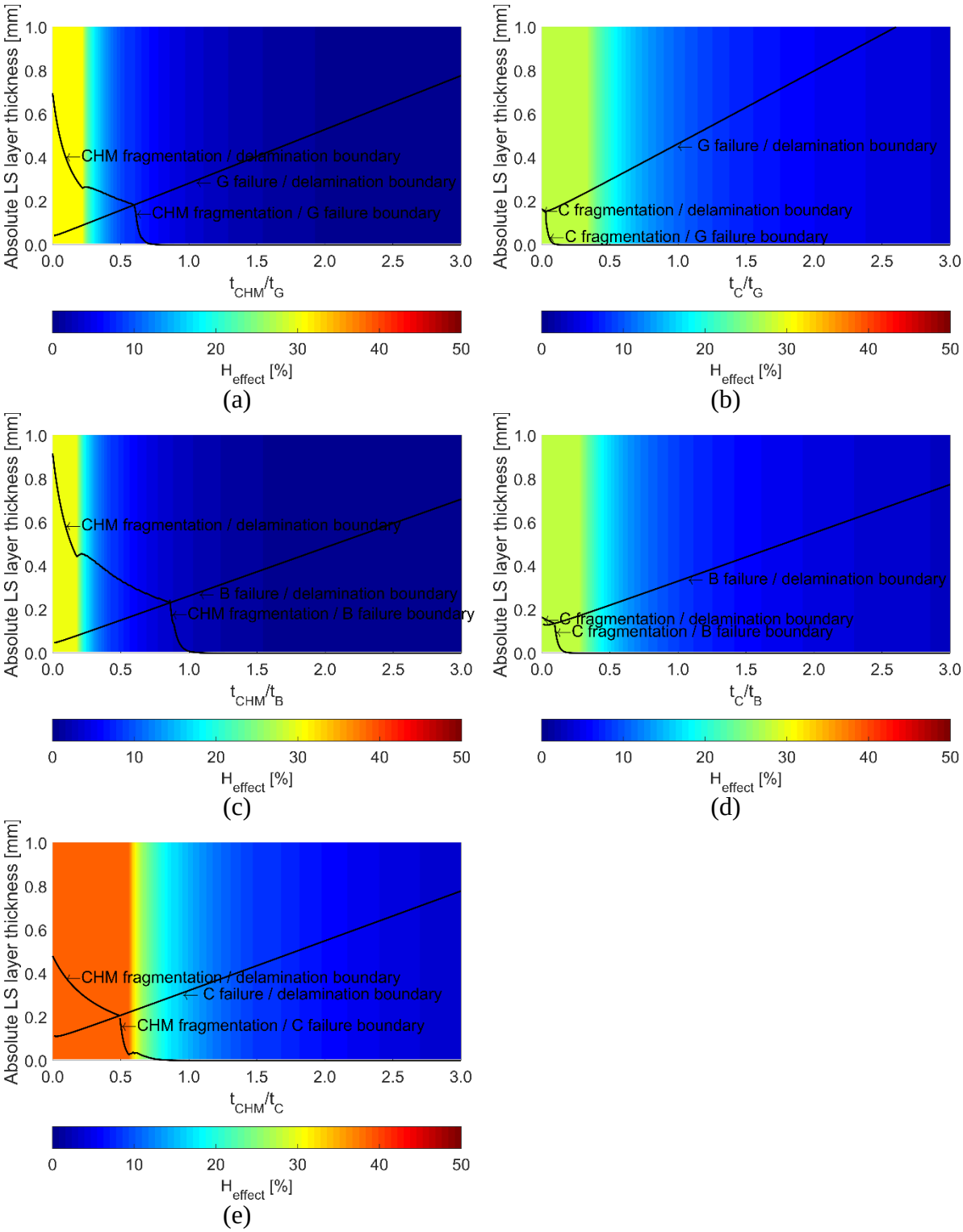

Figure 8 — Damage mode map and distribution of hybrid effect of: (a) HM carbon/glass; (b) ST carbon/glass; (c) HM carbon/basalt; (d) ST carbon/basalt and (e) HM carbon/ST carbon hybrid composites. (For interpretation of the references to colour in this figure legend, the reader is referred to the web version of this article.)

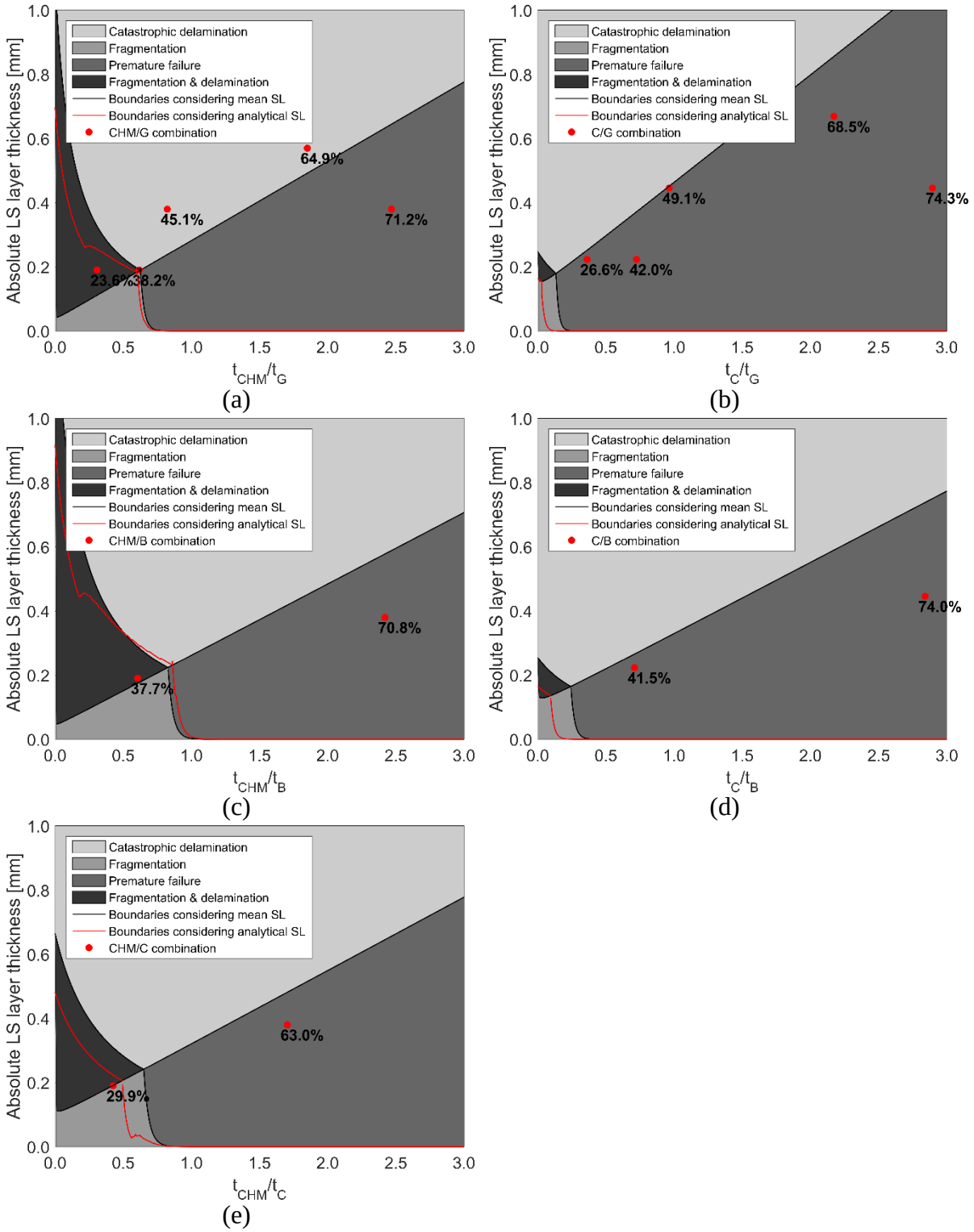

Figure 9 — Predicted damage mode maps with the experimental configurations of: (a) HM carbon/glass; (b) ST carbon/glass; (c) HM carbon/basalt; (d) ST carbon/basalt and (e) HM carbon/ST carbon composites.

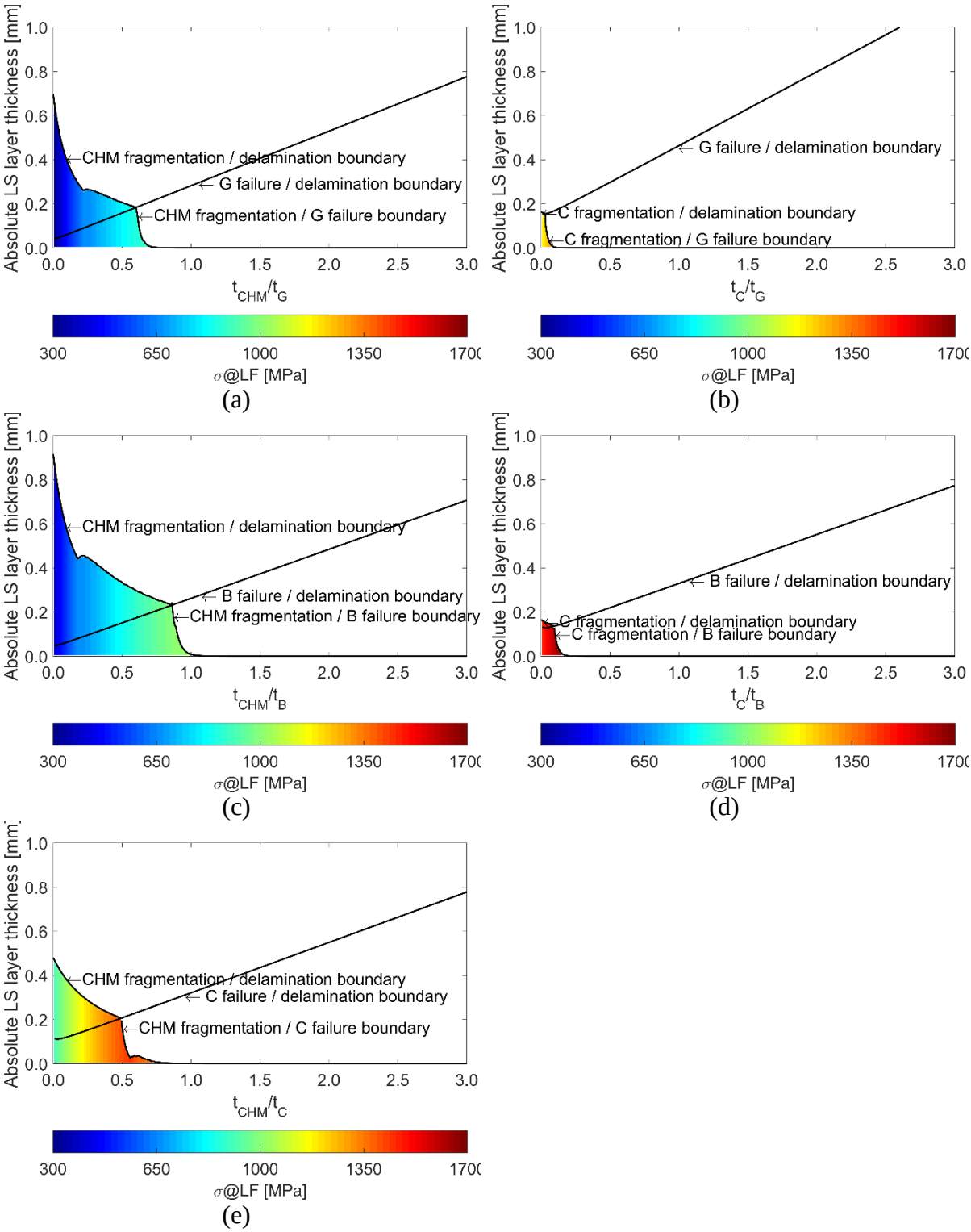

Figure 10 — Damage mode map and distribution of 'yield' stress of: (a) HM carbon/glass; (b) ST carbon/glass; (c) HM carbon/basalt; (d) ST carbon/basalt and (e) HM carbon/ST carbon hybrid composites. (For interpretation of the references to colour in this figure legend, the reader is referred to the web version of this article.)

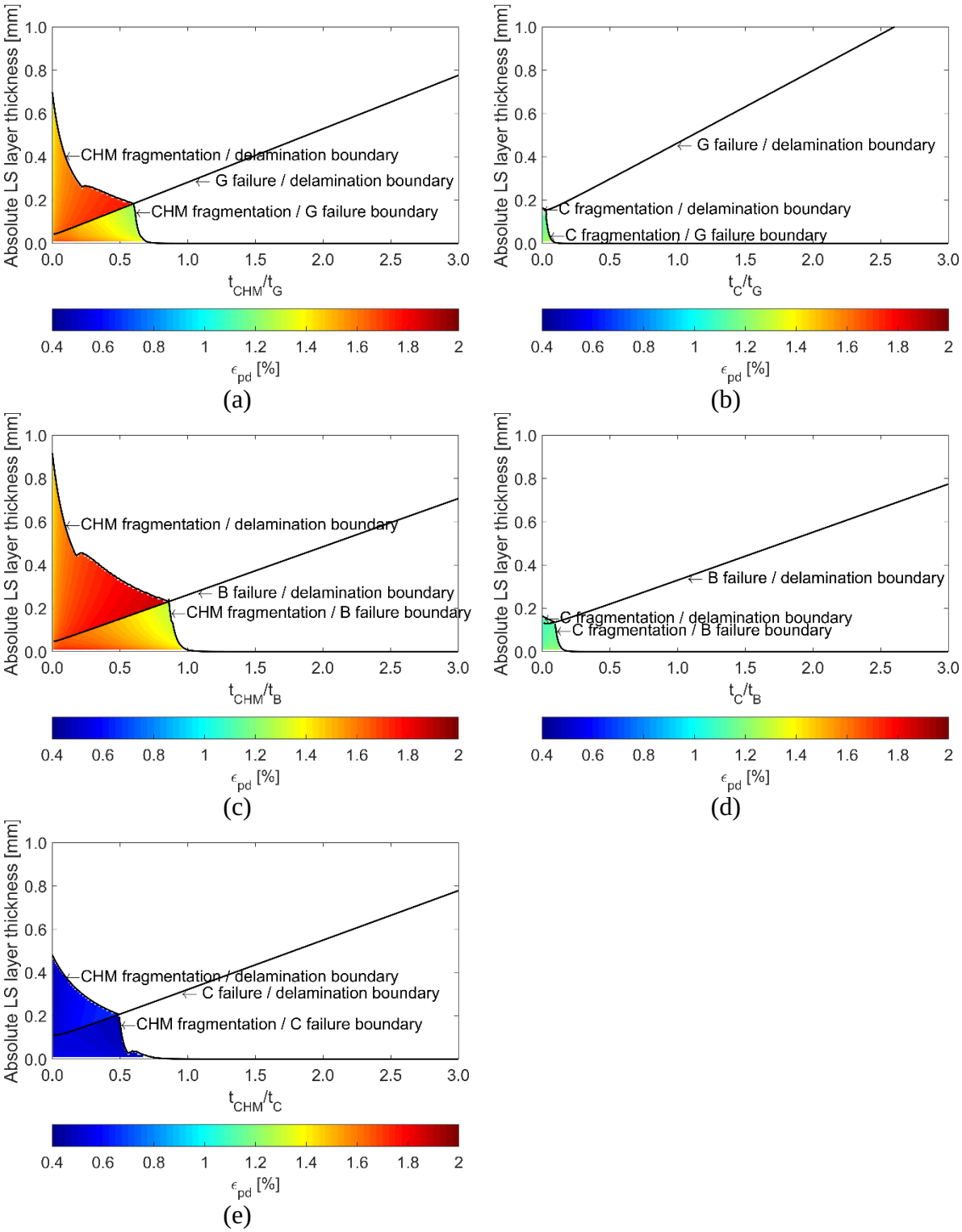

Figure 11 — Damage mode map and distribution of pseudo-ductile strain of: (a) HM carbon/glass; (b) ST carbon/glass; (c) HM carbon/basalt; (d) ST carbon/basalt and (e) HM carbon/ST carbon hybrid composites. (For interpretation of the references to colour in this figure legend, the reader is referred to the web version of this article.)

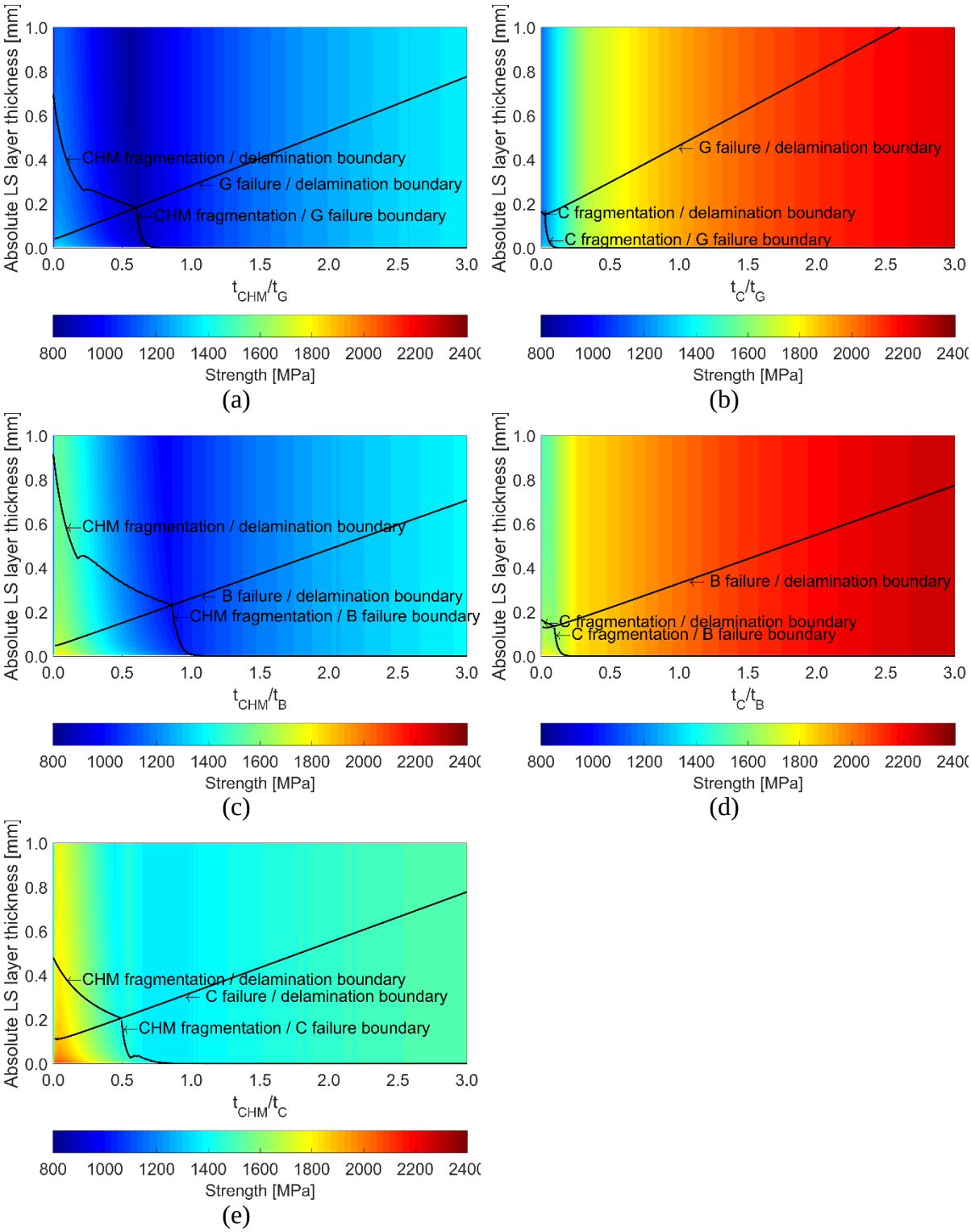

Figure 12 — Damage mode map and distribution of strength of: (a) HM carbon/glass; (b) ST carbon/glass; (c) HM carbon/basalt; (d) ST carbon/basalt and (e) HM carbon/ST carbon hybrid composites. (For interpretation of the references to colour in this figure legend, the reader is referred to the web version of this article.)

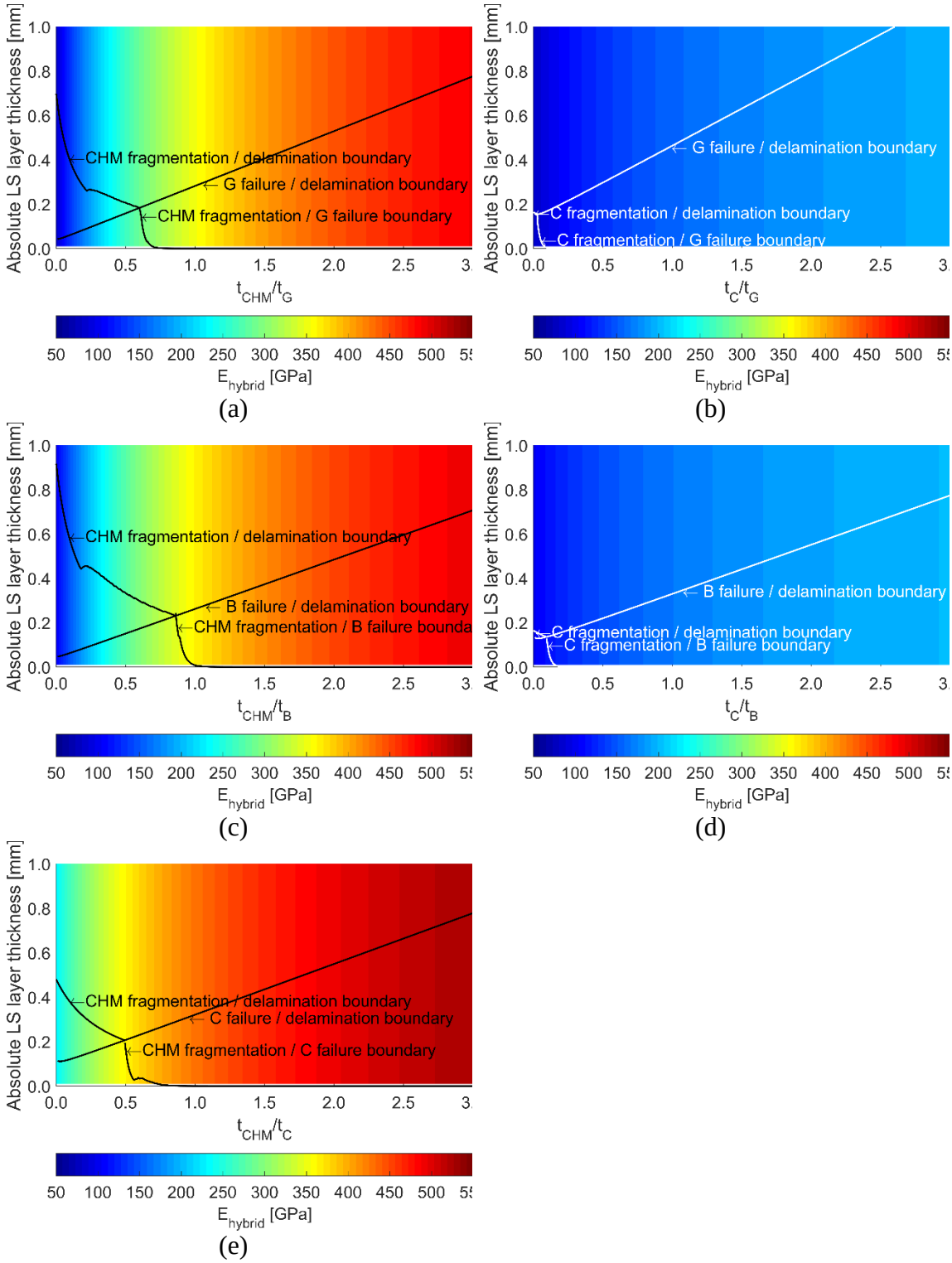

Figure 13 — Damage mode map and distribution of elastic modulus of: (a) HM carbon/glass; (b) ST carbon/glass; (c) HM carbon/basalt; (d) ST carbon/basalt and (e) HM carbon/ST carbon hybrid composites. (For interpretation of the references to colour in this figure legend, the reader is referred to the web version of this article.)